Physics and Imaging in Radiation Oncology 32 (2024) 100675

Contents lists available at ScienceDirect

Physics and Imaging in Radiation Oncology

journal homepage: www.sciencedirect.com/journal/physics-and-imaging-in-radiation-oncology

Original Research Article

Variations in linear energy transfer distributions within a European proton therapy planning comparison of paediatric posterior fossa tumours

Peter Lægdsmand [a,b], Witold Matysiak [c,1], Ludvig P. Muren [a,b], Yasmin Lassen-Ramshad [a], John H. Maduro [c], Anne Vestergaard [a], Roberto Righetto [d], Erik Pettersson [e,f], Ingrid Kristensen [g], Pauline Dutheil [h], Charlotte Demoor-Goldschmidt [h,i], Frances Charlwood [j], Gillian Whitfield [j,k], Marta M. Feijoo [l], Anthony Vela [h], Fernand Missohou [h], Sabina Vennarini [m], Alfredo Mirandola [n], Ester Orlandi [o,p], Barbara Rombi [q], Anneleen Goedgebeur [r], Karen Van Beek [r], Agata Bannink-Gawryszuk [c], Fernando C. Campoo [l], Jacob Engellau [g], Laura Toussaint [a,b,*]

[a] Aarhus University Hospital, Danish Centre for Particle Therapy, Aarhus N, Denmark
[b] Aarhus University, Department of Clinical Medicine, Aarhus N, Denmark
[c] University of Groningen, University Medical Centre Groningen, Department of Radiation Oncology, Groningen, Netherlands
[d] Hospital S. Chiara, APSS, Medical Physics Unit, Trento, Italy
[e] Sahlgrenska University Hospital, Department of Therapeutic Radiation Physics, Gothenburg, Sweden
[f] University of Gothenburg, Department of Medical Radiation Sciences, Gothenburg, Sweden
[g] Skåne University Hospital, Hematology, Oncology and Radiation Physics, Lund, Sweden
[h] Centre Regional Francois Baclesse, Department of Radiation Oncology, Caen, France
[i] Angers University Hospital, Department of Paediatric Oncology, Angers, France
[j] The Christie Proton Beam Therapy Centre, The Christie NHS Foundation Trust, Manchester, United Kingdom
[k] University of Manchester, Royal Manchester Children's Hospital, The Children's Brain Tumour Research Network, Manchester, United Kingdom
[l] Quironsalud, Centro de Protonterapia, Madrid, Spain
[m] Fondazione IRCCS Instituto Nazionale Tumori, Paediatric Radiotherapy Unit, Milano, Italy
[n] CNAO National Center for Oncological Hadrontherapy, Medical Physics Unit, Clinical Department, Pavia, Italy
[o] CNAO National Center for Oncological Hadrontherapy, Clinical Department, Pavia, Italy
[p] University of Pavia, Department of Clinical, Surgical, Diagnostic, and Pediatric Sciences, Pavia, Italy
[q] Proton Therapy Centre, Hospital S. Chiara, APSS, Trento, Italy
[r] Particle UZLeuven, Department of Radiation Oncology, Leuven, Belgium

ARTICLE INFO

Keywords:
Proton therapy
Linear Energy Transfer
Relative Biological Effectiveness
Paediatric
Posterior fossa tumours
Brainstem
Spinal cord

ABSTRACT

Background and Purpose: Radiotherapy for paediatric posterior fossa tumours may cause complications in the brainstem and upper spinal cord due to high doses. With proton therapy (PT) this risk may increase due to higher relative biological effectiveness (RBE) from elevated linear energy transfer (LET). This study assesses variations in LET in the brainstem and spinal cord in proton treatment plans from European centres.
Materials and Methods: Ten European PT centres using spot-scanning PT planned two paediatric posterior fossa cases: One overlapping partly with the brainstem and upper spinal cord, prescribed 54 Gy(RBE), and the second wrapping around these organs, prescribed 59.4 Gy(RBE). Dose-averaged LET distributions were assessed in volumes of the brainstem and spinal cord irradiated to over 50 Gy(RBE = 1.1). The maximum hinge angle effect on near-maximum RBE-weighted doses using the Unkelbach RBE model was also investigated.
Results: In the first case, the mean LET in brainstem volumes receiving more than 50 Gy(RBE = 1.1) ranged from 2.8 keV/μm to 3.6 keV/μm across centres (median: 3.3 keV/μm). In the second case, treatment plans showed a narrower range of mean LET in the brainstem, from 2.5 keV/μm to 2.8 keV/μm (median: 2.7 keV/μm). There was no statistically significant impact of the maximum hinge angle.
Conclusions: LET distributions vary across centres due to different techniques but are also influenced significantly by factors like shape and position of the target volume.

* Corresponding author at: Danish Centre for Particle Therapy, Palle Juul-Jensens Boulevard 25, 8200 Aarhus N, Denmark.
E-mail address: lautou@rm.dk (L. Toussaint).
[1] Present adress: Mayo Clinic, Department of Radiation Oncology, Rochester, USA.

https://doi.org/10.1016/j.phro.2024.100675
Received 29 April 2024; Received in revised form 10 October 2024; Accepted 12 November 2024
Available online 17 November 2024

1. Introduction

Central nervous system tumours, the most common solid cancers in children [1], are often located in the posterior fossa and require radiotherapy for cure. Concerns about brainstem and upper cervical spinal cord injuries arise in treating this location [2–5]. Proton Therapy (PT) has increasingly been used for paediatric brain tumour radiotherapy [6,7]. Compared to conventional photon-based radiotherapy, PT can reduce the normal tissue volumes irradiated to low-to-medium doses [8]. This improves normal tissue sparing, potentially reducing risks for radiation-related complications. PT has in particular been shown to mitigate loss of cognitive performance and endocrine function compared to conventional radiotherapy [9,10].

The preclinical correlation between Relative Biological Effectiveness (RBE) and Linear Energy Transfer (LET) suggests an increased risk of injury in volumes exposed to both high doses and high LET [11], however, a constant RBE of 1.1 is recommended and used globally as a tool for prescribing and assessing PT dose distributions [11,12]. Phenomenological models, based on *in vitro* data, parameterize RBE prediction by considering tissue alpha–beta ratio and LET. *In vivo* endpoint experiments, which may more accurately predict clinical effects, have also confirmed a LET-RBE correlation [13–16]; though further data is needed [17]. Recent studies examining the correlation between diagnostic imaging changes and LET in high-dose volumes presented conflicting findings: Some suggested a statistically significant correlation [18–20], but a recent study showed that an appropriate statistical model failed to confirm this result [21]. A case-control study of symptomatic brainstem necrosis indicated a correlation with LET but lacked statistical significance due to a limited number of cases [22,23]. Overall, it is still uncertain how large the clinical significance of the effect is.

PT delivery techniques are evolving, with spot-scanning delivery now offering improved conformality in dose distribution over the older passive scattering delivery [24,25]. However, this development leads to more modulated distributions of both dose and LET [25]. Studies have investigated how field configurations and target position affect the LET distribution for passive scattering [26] and spot-scanning delivery [27], including their sensitivity to range uncertainties [28].

A recent comparative analysis of treatment planning practices

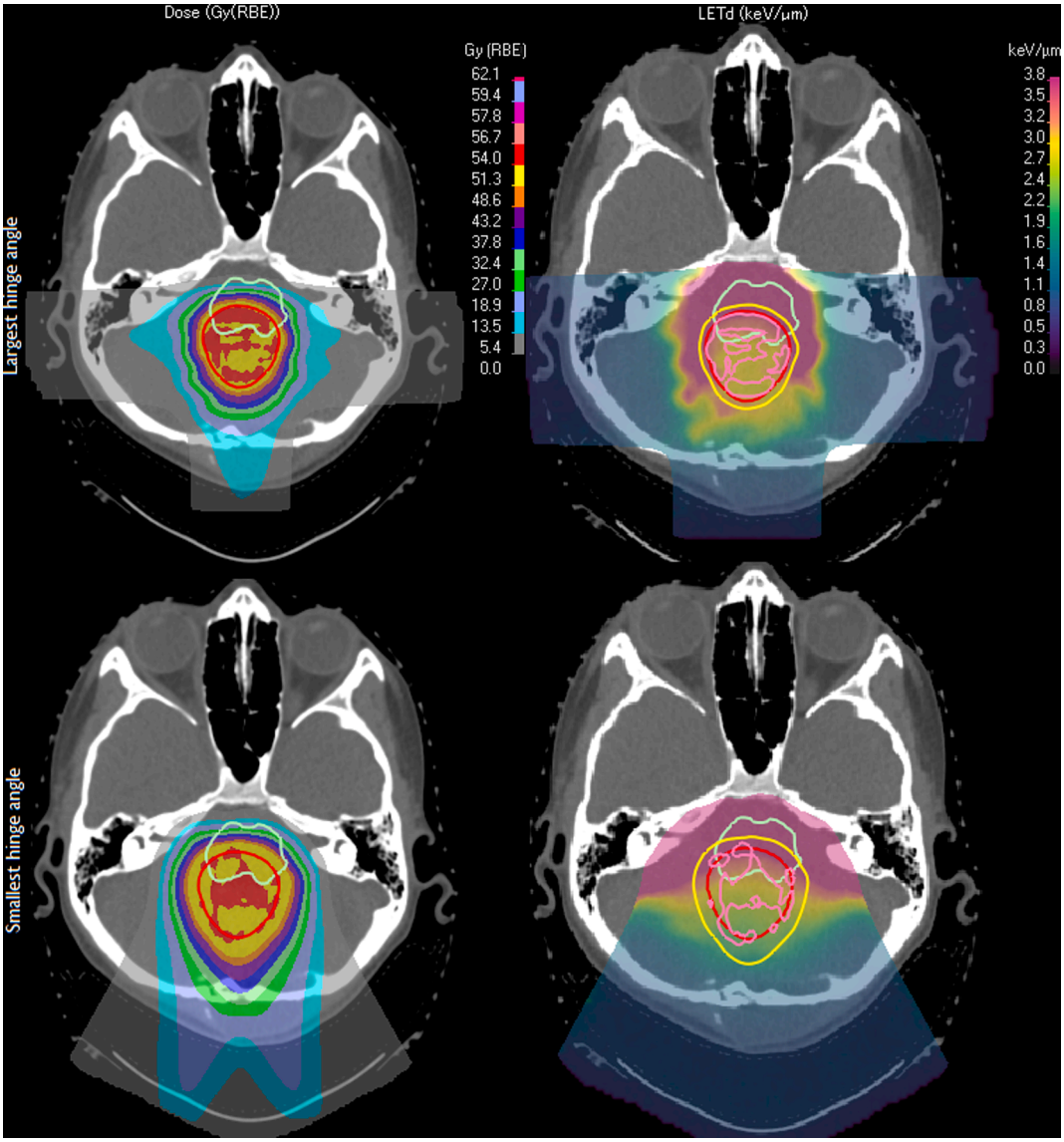

Fig. 1. Dose (Gy(RBE)) and LET (keV/µm) distributions for two of the ATRT plans—with the highest and lowest hinge angles. Colourwash scale shown in the upper right corner. The contour of CTV is shown in red and the brainstem in cyan. In the LET map, the 50 Gy(RBE) and 54 Gy(RBE) volumes are demarcated by the yellow and pink lines, respectively. (For interpretation of the references to colour in this figure legend, the reader is referred to the web version of this article.)

among European centres specialised in spot-scanning PT for children revealed considerable variations in dose-volume parameters [29], with variations arising from the choice of field configurations, optimisation strategies, normal tissue constraints and prioritisation, RBE mitigation techniques, and robustness evaluation against range and setup uncertainties [29]. However, the assessment of LET distributions and their potential impact on RBE has not yet become a standard clinical practice, despite being recognized as a concern in PT [12]. Although some studies have already investigated the effect of different field configurations on the LET distribution in posterior fossa treatment plans, there is a lack of knowledge regarding the cross-institutional variation in LET distributions. Consequently, this study aimed to quantify and analyse variations in LET distributions within the brainstem and upper spinal cord in posterior fossa cases across European centres reflecting their unique clinical practice.

2. Materials and methods

2.1. Clinical cases and centre participation

Ten European spot-scanning PT centres participated in a treatment planning comparison [29]. The centres planned two representative paediatric posterior fossa cases based on their clinical practices: firstly, an Atypical Teratoid Rhabdoid Tumour (ATRT, Fig. 1) overlapping with the dorsal side of the brainstem prescribed 54 Gy(RBE) (1.8 Gy(RBE)/fraction). Secondly, an Ependymoma tumour (Fig. 2) wrapping around the brainstem, prescribed 54 Gy(RBE); and a boost (brainstem and spinal cord cropped out of the clinical target volume (CTV)) to a total dose of 59.4 Gy(RBE). Both CTVs extended partially into the upper spinal cord (spinal cord C1). The cases represent the most common indications at risk of brainstem injury [5], and both have prescribed doses near the brainstem tolerance, even for small volumes [2,5]. The patient also had an oedema and three metal implants on the posterior part of the skull as shown in supplementary figure 1.

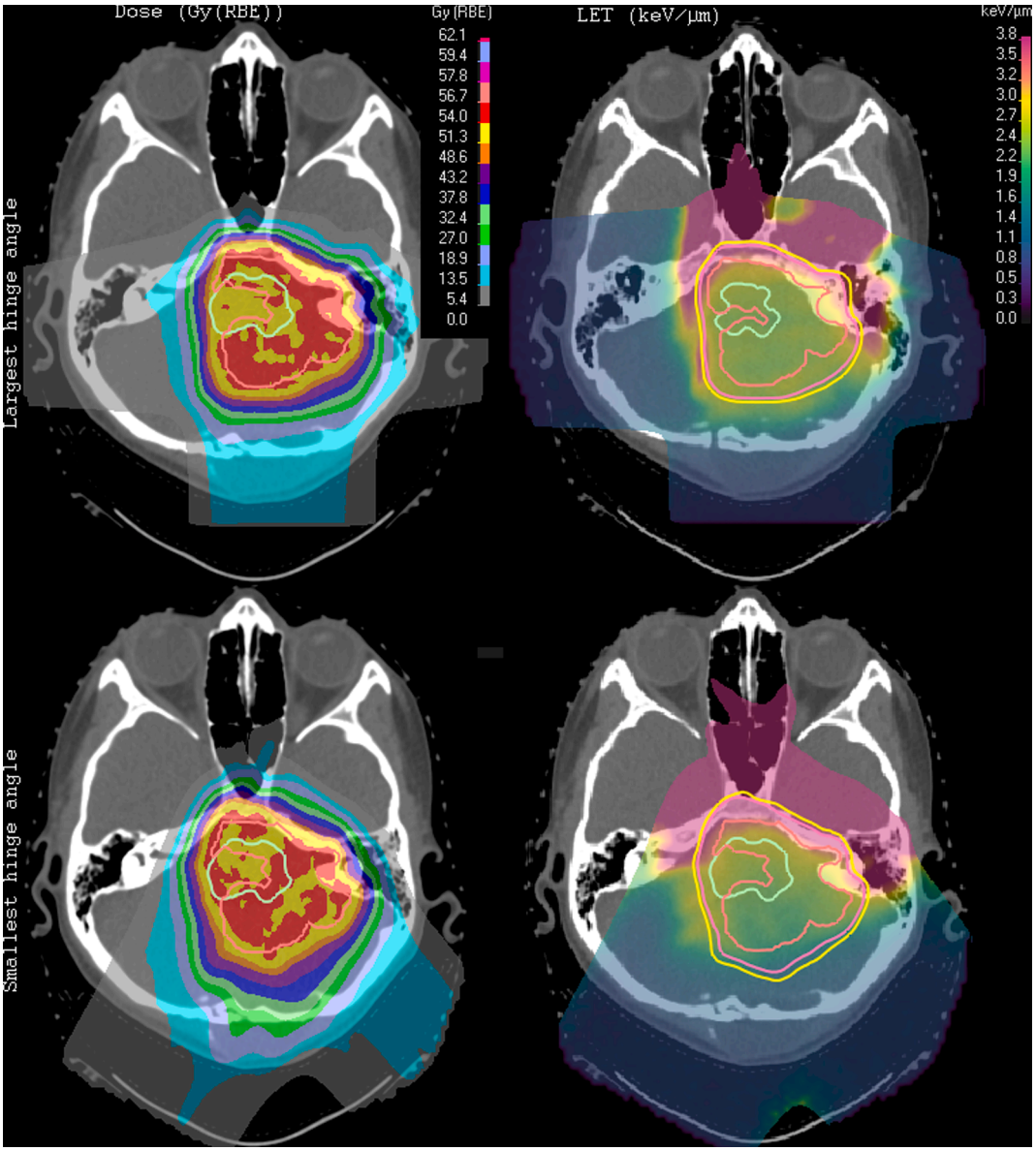

Fig. 2. Dose (Gy(RBE)) and LET (keV/µm) distributions for the Ependymoma plans with the highest and lowest hinge angle. The colorwash scale is shown in the upper right corner. The contour of CTV is shown in red and the brainstem in cyan. In the LET map, the 50 Gy(RBE) and 54 Gy(RBE) volumes are demarcated by the yellow and pink lines, respectively. (For interpretation of the references to colour in this figure legend, the reader is referred to the web version of this article.)

Anonymized computed tomography images with CTVs, and normal tissue contours were distributed to the centres in DICOM format to allow treatment planning in the centres' respective clinical treatment planning systems (TPSs). All centres robustly optimised their plans, but with varying range and position margins, and number of uncertainty scenarios [29]. This is also shown in the variation of the individual dose distributions submitted in supplementary figure 2.

The treating institution and the patient's guardians approved the use of the patient's anonymized data.

2.2. LET distribution evaluation

LET was scored for primary and secondary protons, normalised to water or unit-density tissue, and dose-averaged [30] for all treatment plans by the ten participating centres, using their respective beamline Monte Carlo implementations in Raystation 11B, TOPAS, or GATE. The LET variation across these calculation methods was shown to be at most 10–15 % in a phantom study [31]. LET distributions for each centre were calculated on the same voxel grid as their submitted dose distributions. Monte Carlo calculation uncertainties are reported in Table S1. For the ependymoma plan, LET distributions were calculated by dose-averaging the LET distribution for the main plan and the boost plan, using the TPS dose distribution. LET-volume histograms (LVHs) were evaluated inside the 50 Gy(RBE), the 54 Gy(RBE), or for the ependymoma case, the 55 Gy (RBE) isodose overlapping with either the spinal cord or the brainstem. These thresholds, though somewhat arbitrary, align with previous studies of LET in the brainstem [22] and reflect that the risk to the brainstem and spinal cord primarily is associated with doses exceeding these values [2,5,32]. Welch's *t*-test was used to compare the mean LET between the two cases.

2.3. Variable RBE weighted dose evaluation

We evaluated variable RBE weighted dose distributions in the brainstem and spinal cord C1 with the Unkelbach model [33], which assumes a linear dependency of RBE on LET and that the RBE is 1.1 at the centre of a standard spread-out Bragg peak (where LET = 2.5 keV/μm). We chose this model because it is easier to interpret its relation to LET than phenomenological models, where RBE also depends on the alpha–beta ratio. Supplementarily, the McNamara model was used with an alpha–beta ratio of 2 Gy for the organs at risk [34].

2.4. Impact of field angles

The maximum hinge angle, i.e. the largest angle between any two fields in a plan, can potentially be linked to elevated LET by the separation of distal edges [11]. We calculated this angle for each plan to study its effect on the LET distribution. The dependency of the brainstem and spinal cord C1 D2% under the Unkelbach model on the hinge angle parameter was then investigated, as the near max dose is considered a significant risk factor for brainstem and spinal cord injury. The correlation with the hinge angle was tested using the Pearson correlation coefficient. In this analysis, only the plans with distal edges in the given organ were considered.

3. Results

3.1. LET distributions

In the ATRT treatment plans, the average LET within the 50 Gy(RBE) isodose in the brainstem ranged from 2.8 keV/μm to 3.6 keV/μm, as detailed in Table 1 and Fig. 3. Notably, all but one treatment plan exhibited a mean LET higher than 3 keV/μm. Conversely, this single plan presented the highest LET in the spinal cord, attributed to all the fields entering from the superior direction with edges extending into the spinal cord, whereas other centres used fields ending in the brainstem. The ependymoma treatment plans showed a comparatively lower mean LET within the 50 Gy(RBE) isodose in the brainstem, ranging from 2.5 keV/μm to 2.8 keV/μm across institutions. Welsch *t*-test showed a significant difference ($p < 0.001$) in mean LET in the brainstem in the 50 Gy(RBE) threshold between the two cases. A similar trend was observed for the spinal cord C1, as shown in Table 1, for which, the *t*-test also showed a significant difference in the mean LET ($p = 0.024$). Supplementary figure 3 presents the individual LET distributions, while Table S2 provides the individual numerical values.

3.2. Variable RBE weighted doses

Fig. 4 highlights a pronounced RBE-weighted dose enhancement using the Unkelbach model over a fixed RBE of 1.1 in the ATRT case, with increase in brainstem D2% ranging from 1.3 % to 6.0 %, while enhancement in the spinal cord C1 only ranged from 0.8 % to 3.8 %. In the ependymoma plans, the increase was smaller, ranging only from 0.2 % to 2.1 % for the brainstem and from −0.2 % to 1.8 % for the spinal cord C1. Regardless of variable RBE, the ependymoma case had higher maximum doses and dose variations across plans due to its higher prescribed total dose. The McNamara model predicted increased RBE-weighted doses with increased range (Supplementary Figure 4). Individual RBE-weighted doses are shown in Table S2.

3.3. Impact of field configurations

Most of the ATRT and ependymoma treatment plans employed a combination of posterior and posterior oblique treatment fields, with the majority being coplanar or near-coplanar (detailed field configurations shown in Table S3). Among the ATRT treatment plans, the maximum hinge angle ranged from 60 to 180 degrees. A slight trend towards a lower increase in LET-weighted D2% in the brainstem was observed in plans with larger hinge angles, as depicted in Fig. 5, although no statistically significant correlation was identified (Pearson correlation coefficient: −0.45, $p = 0.22$, excluding the plan with distal edges pointed towards the spinal cord). The increase in the LET-weighted D2% in the spinal cord C1 showed no correlation with the hinge angle with a Pearson correlation coefficient of 0.15 ($p = 0.71$). In the main ependymoma treatment plans, the hinge angle ranged from 70 to 168 degrees, and showed no correlation with brainstem or spinal cord C1 D2%.

4. Discussion

Our investigation into LET distributions in paediatric posterior fossa plans across European PT institutions revealed noteworthy variations in the high-dose regions of the brainstem and upper spinal cord. These variations were especially prominent for the ATRT case. Although the clinical significance of the LET variations is still uncertain, the Unkelbach model, which predicts lower RBE than most empirical models [35], predicted RBE dose boosts that were comparable to the physical variations shown in a previous study [29].

Hahn et al. [31] demonstrated that even between harmonised calculation methods, differences in LET in the worst case approached 15 %. Importantly, the variation in variable RBE-weighted dose was similar to the variation in the physical dose calculated across institutions, indicating that the LET uncertainty remains within clinically acceptable levels. Even accounting for this variability, the differences observed in our study are considerable in size.

The higher mean LET across institutions in both organs for the ATRT across institutions also emphasises the importance of the geometrical shape and position of the CTV, affecting whether distal edges are directed inside these structures. This is also consistent with the study by Fjæra et al., where the scenario with the target partly overlapping with the brainstem, akin to the ATRT case, also showed higher LET in the brainstem than the full overlap scenario, akin to the ependymoma case. The RBE percentage increase of the maximum dose when applying a

Table 1
Median and range of mean LET within the 50 Gy(RBE) isodose overlap with the brainstem, spinal cord C1 or CTV, and the range of the relative increase in D2% from applying the Unkelbach model compared to RBE = 1.1 across the ten treatment plans.

	ATRT			Ependymoma		
	Brainstem	Spinal cord C1	CTV	Brainstem	Spinal cord C1	CTV
LET range (keV/μm)	[2.8;3.6]	[2.7;3.8]	[2.7;3.0]	[2.5;2.8]	[2.5;3.0]	[2.5;2.7]
LET Median (keV/μm)	3.3	3.0	2.9	2.7	2.8	2.7
Unkelbach D2% enhancement range (%)	[1.3;6.0]	[0.8;3.8]		[0.2;2.1]	[-0.2;1.8]	
Unkelbach D2% enhancement median (%)	3.7	1.7		1.2	1.0	

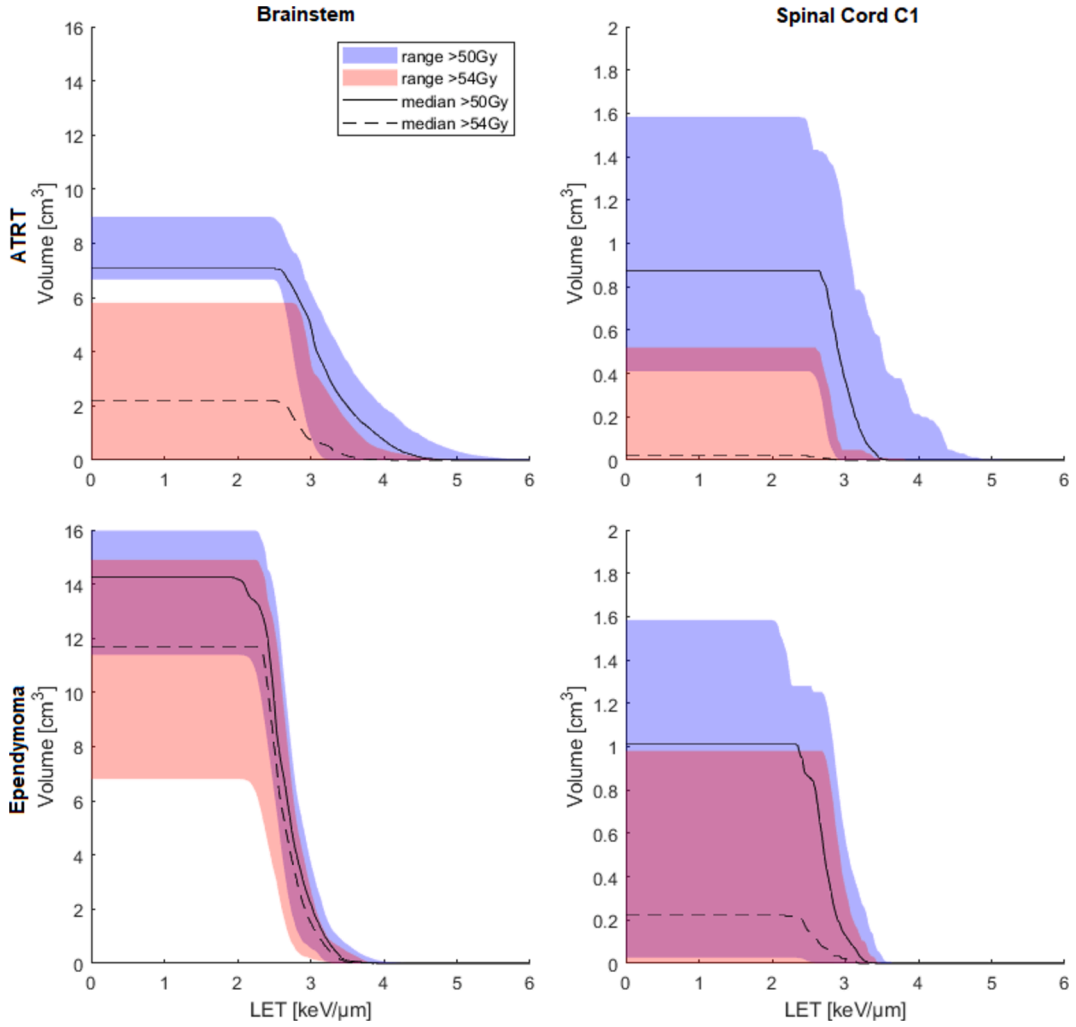

Fig. 3. LVH for the brainstem (left) and the C1 segment of the spinal cord (right) for the ATRT plans (upper), and the ependymoma plans (lower) with absolute volume of the region of interest. The blue-shaded region shows the range of LVHs across the plans inside the overlap of the 50 Gy(RBE) isodose and the OAR contour, while the red region shows the LVH inside the overlap with the 54 Gy(RBE) isodose. The lines show the median LVH across the centres. (For interpretation of the references to colour in this figure legend, the reader is referred to the web version of this article.)

model similar to Unkelbach was 2.1 % for the half-overlap scenario and 1.6 % for the full-overlap scenario, whereas the median across centres was more different for the two cases in the current study (3.7 % and 1.2 % respectively). The participating centres reported avoiding distal edges in the brainstem as part of their clinical practice [29], but in the ATRT case, it was not possible to avoid them either in the brainstem or spinal cord. Yet, this case still showed the largest variation in LET across institutions, so it could be interesting to optimise LET distributions in such cases.

In the study by Giantsoudi et al. [26], the ependymoma cases investigated were similarly characterised by CTV overlapping with the dorsal side of the brainstem, as the ATRT case in our study, albeit utilising the passive scattering technique. They assessed median LET in the brainstem within the CTV for various field configurations. Specifically, dose-sparing techniques resulted in a median LET of 3.0 keV/μm for three-field and 2.9 keV/μm for two-field configurations, which aligns with our findings in the ATRT case, where the mean LET ranged from 2.8 to 3.6 keV/μm in the 50 Gy(RBE) isodose.

Ensuring a minimum value of the hinge angle may be used as a strategy by some institutions to reduce hotspots in the LET distribution, as it can increase the spacing between distal edges [11,12]. Our study did not show this effect of the hinge angle, but this could also have been

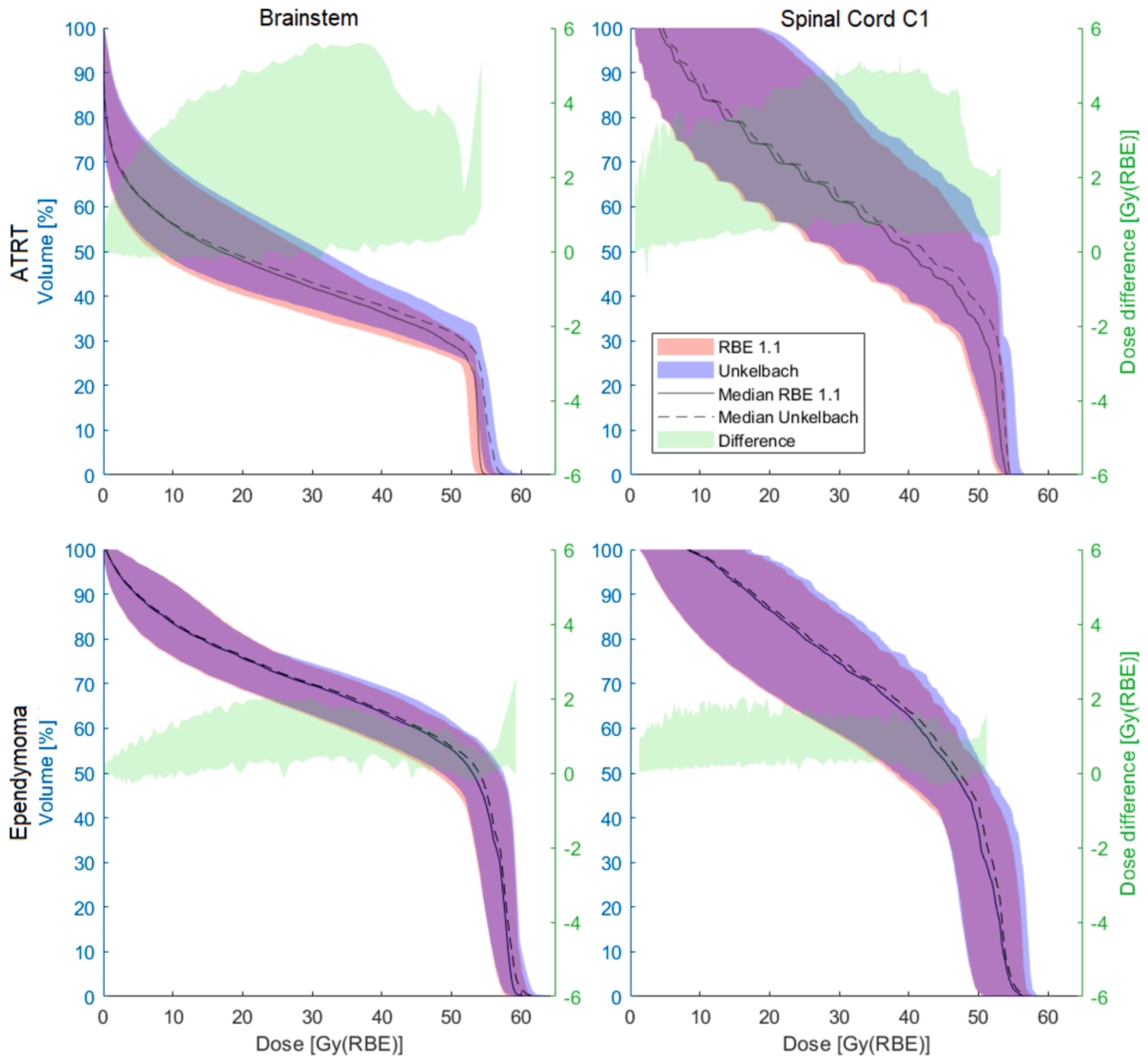

Fig. 4. Dose-volume-histograms for the brainstem (left) and spinal cord C1 segment (right) in the ATRT plans (upper) and Ependymoma plans (lower). Red shaded region shows the range of DVH values for the plans with a constant RBE, while the blue shaded region shows the DVH values weighted with a variable RBE under the Unkelbach model. The green shaded region shows the range of difference in RBE weighted dose between using the Unkelbach model and the RBE = 1.1. (For interpretation of the references to colour in this figure legend, the reader is referred to the web version of this article.)

influenced by the fact that all plans used quite large angular spacing. Furthermore, LET hotspots could be caused by a few heavily weighted spots located at a distal edge of one of the fields [25], and the steepness of the dose-fall off at the distal edges could also have affected the LET [26]. We were not able to do an exhaustive analysis of treatment planning parameters affecting the LET distribution, but it emphasises the complexity of the unique optimization and prioritisation process used by each institution, and therefore the value of a standardised LET calculation, that facilitates an objective assessment of individual plans beyond heuristics. Vertex field configurations could also reduce the LET in the brainstem [27]. However, depending on the exact extent of the CTV, the cranial field could also result in increased LET to the high-dose region of the inferior part of the brainstem or the cervical spinal cord for which the tolerance dose is presumed to be lower than the brainstem [4,29].

Concerns about RBE have led more centres to explore reducing LET hotspots in critical organs at risk, using spot-wise optimization, now under testing in a phase I trial (NCT03750513). However, when evaluating LET distributions of treatment plans, it is important to also evaluate the effect of range and set-up uncertainties. It has been shown that the variation in LET in organs at risk across robust uncertainty scenarios can be considerable, especially for treatment plans with dose and LET distributions optimised only for the nominal scenario [28,36]. A limitation of the current study is therefore also that only nominal dose and LET distributions were collected and analysed.

While the Unkelbach model was used to translate the potential influence of LET distributions, phenomenological models tend to predict higher RBE than Unkelbach for low alpha–beta ratios [35] (supplementary figure 3). However, it is still uncertain whether those estimates are a good surrogate for RBE for clinical endpoints, as clinical studies face sample size challenges [23,37], and predictions of these models still vary widely [38]. Furthermore, a recent *in vitro* modelling study has shown that another quantity, effective Q, may correlate significantly better with RBE compared to LET [39]. Thus, caution is needed when interpreting the clinical implications of RBE predictions.

In conclusion, the LET distributions in the brainstem and upper spinal cord varied considerably across institutions for the two cases. Our study also emphasised the influence of target shape and position, with one geometry making placement of distal field edges in the brainstem or upper spinal cord unavoidable, and another geometry allowing the distal edges beyond these organs.

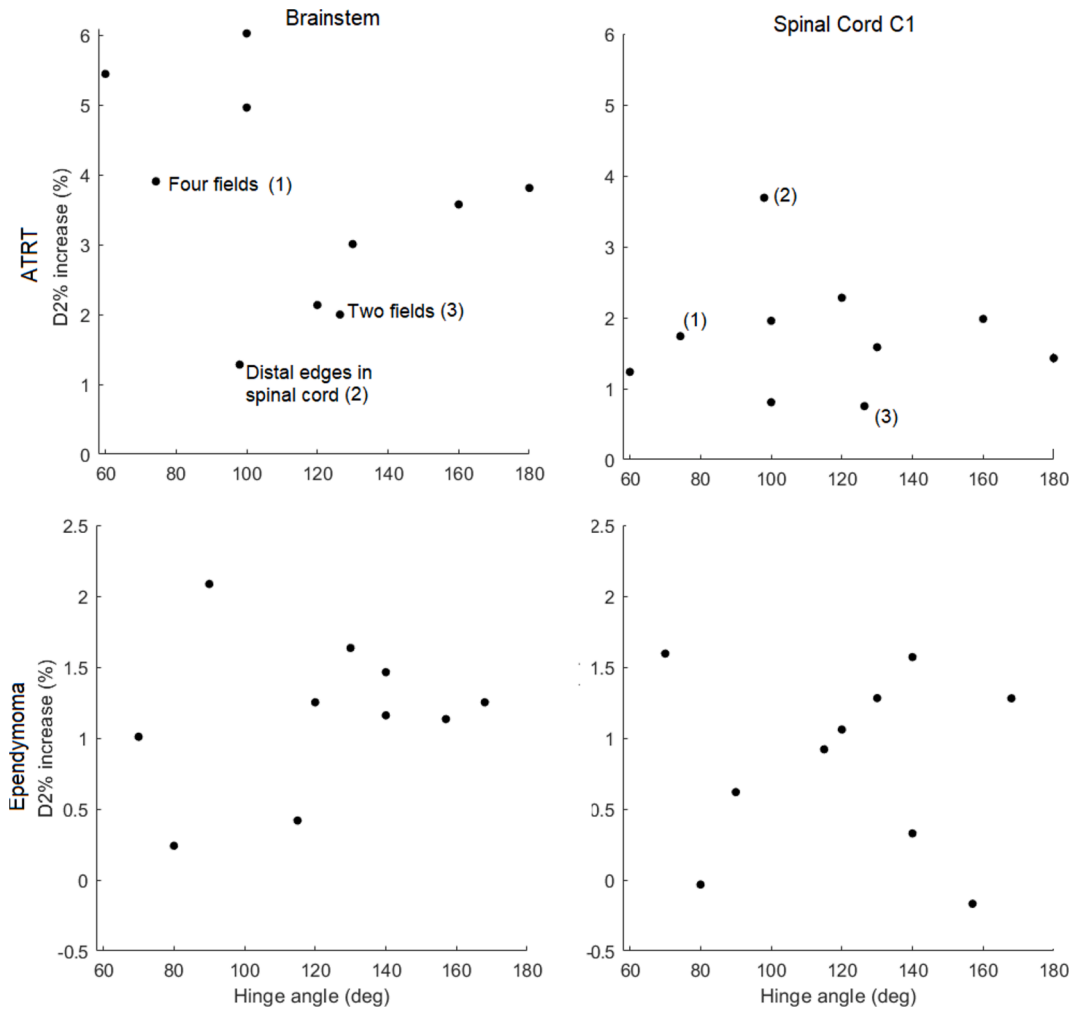

Fig. 5. Hinge angle and increment in D2% of the brainstem when weighting dose with the Unkelbach RBE compared to 1.1 of each of the ATRT treatment plans. Each dot represents a plan from a participating institution. Three plans with unique field configurations are indicated.

CRediT authorship contribution statement

Peter Lægdsmand: Conceptualization, Methodology, Software, Formal analysis, Investigation, Data curation, Writing – original draft, Writing – review & editing, Visualization, Supervision, Project administration. **Witold Matysiak:** Conceptualization, Methodology, Software, Investigation, Data curation, Writing – review & editing. **Ludvig P. Muren:** Investigation, Writing – review & editing, Visualization, Supervision. **Yasmin Lassen-Ramshad:** Conceptualization, Investigation, Resources, Writing – review & editing. **John H. Maduro:** Conceptualization, Investigation, Writing – review & editing. **Anne Vestergaard:** Investigation, Writing – review & editing. **Roberto Righetto:** Investigation, Writing – review & editing. **Erik Pettersson:** Investigation, Writing – review & editing. **Ingrid Kristensen:** Investigation, Writing – review & editing. **Pauline Dutheil:** Investigation, Writing – review & editing. **Charlotte Demoor-Goldschmidt:** Investigation, Writing – review & editing. **Frances Charlwood:** Investigation, Writing – review & editing. **Gillian Whitfield:** Investigation, Writing – review & editing. **Marta M. Feijoo:** Investigation, Writing – review & editing. **Anthony Vela:** Investigation, Writing – review & editing. **Fernand Missohou:** Investigation, Writing – review & editing. **Sabina Vennarini:** Investigation, Writing – review & editing. **Alfredo Mirandola:** Investigation, Writing – review & editing. **Ester Orlandi:** Investigation, Writing – review & editing. **Barbara Rombi:** Investigation, Writing – review & editing. **Anneleen Goedgebeur:** Investigation, Writing – review & editing. **Karen Van Beek:** Investigation, Writing – review & editing. **Agata Bannink-Gawryszuk:** Investigation, Writing – review & editing. **Fernando C. Campoo:** Investigation, Writing – review & editing. **Jacob Engellau:** Investigation, Writing – review & editing. **Laura Toussaint:** Conceptualization, Methodology, Investigation, Writing – review & editing, Supervision.

Declaration of competing interest

The authors declare that they have no known competing financial interests or personal relationships that could have appeared to influence the work reported in this paper.

The author Ludvig Muren is an Editor-in-Chief for *Physics and Imaging in Radiation Oncology* and was not involved in the editorial review or the decision to publish this article.

Acknowledgments

The authors are grateful to Dr. Adam Aitkenhead, and Dr. Erik Almhagen for providing LET distributions for treatment plans from one and two centres, respectively.

We also thank the Danish Centre for Particle Therapy (Aarhus, Denmark) for financial support of this project and the workshop that it was connected with.

Appendix A. Supplementary material

Supplementary data to this article can be found online at https://doi.org/10.1016/j.phro.2024.100675.

References

[1] Steliarova-Foucher E, Colombet M, Ries LAG, Moreno F, Dolya A, Bray F, et al. International incidence of childhood cancer, 2001–10: a population-based registry study. Lancet Oncol 2017;18:719–31. https://doi.org/10.1016/S1470-2045(17)30186-9.

[2] Indelicato DJ, Flampouri S, Rotondo RL, Bradley JA, Morris CG, Aldana PR, et al. Incidence and dosimetric parameters of pediatric brainstem toxicity following proton therapy. Acta Oncol 2014;53:1298–304. https://doi.org/10.3109/0284186X.2014.957414.

[3] Gentile MS, Yeap BY, Paganetti H, Goebel CP, Gaudet DE, Gallotto SL, et al. Brainstem injury in pediatric patients with posterior fossa tumors treated with proton beam therapy and associated dosimetric factors. Int J Radiat Oncol Biol Phys 2018;100:719–29. https://doi.org/10.1016/j.ijrobp.2017.11.026.

[4] Haas-Kogan D, Indelicato D, Paganetti H, Esiashvili N, Mahajan A, Yock T, et al. National cancer institute workshop on proton therapy for children: considerations regarding brainstem injury. Int J Radiat Oncol Biol Phys 2018;101:152–68. https://doi.org/10.1016/j.ijrobp.2018.01.013.

[5] Upadhyay R, Liao K, Grosshans DR, McGovern SL, McAleer MF, Zaky W, et al. Quantifying the risk and dosimetric variables of symptomatic brainstem injury after proton beam radiation in pediatric brain tumors. Neuro-Oncol 2022;24:1571–81. https://doi.org/10.1093/neuonc/noac044.

[6] Journy N, Indelicato DJ, Withrow DR, Akimoto T, Alapetite C, Araya M, et al. Patterns of proton therapy use in pediatric cancer management in 2016: an international survey. Radiother Oncol 2019;132:155–61. https://doi.org/10.1016/j.radonc.2018.10.022.

[7] Indelicato DJ, Merchant T, Laperriere N, Lassen Y, Vennarini S, Wolden S, et al. Consensus report from the stockholm pediatric proton therapy conference. Int J Radiat Oncol Biol Phys 2016;96:387–92. https://doi.org/10.1016/j.ijrobp.2016.06.2446.

[8] Newhauser WD, Zhang R. The physics of proton therapy. Phys Med Biol 2015;60:R155–209. https://doi.org/10.1088/0031-9155/60/8/R155.

[9] Eaton BR, Esiashvili N, Kim S, Patterson B, Weyman EA, Thornton LT, et al. Endocrine outcomes with proton and photon radiotherapy for standard risk medulloblastoma. Neuro-Oncol 2016;18:881–7. https://doi.org/10.1093/neuonc/nov302.

[10] Kahalley LS, Ris MD, Grosshans DR, Okcu MF, Paulino AC, Chintagumpala M, et al. Comparing intelligence quotient change after treatment with proton versus photon radiation therapy for pediatric brain tumors. J Clin Oncol 2016;34:1043–9. https://doi.org/10.1200/JCO.2015.62.1383.

[11] Paganetti H, Blakely E, Carabe-Fernandez A, Carlson DJ, Das IJ, Dong L, et al. Report of the AAPM TG-256 on the relative biological effectiveness of proton beams in radiation therapy. Med Phys 2019;46:e53–78. https://doi.org/10.1002/mp.13390.

[12] Heuchel L, Hahn C, Pawelke J, Sørensen BS, Dosanjh M, Lühr A. Clinical use and future requirements of relative biological effectiveness: survey among all European proton therapy centres. Radiother Oncol 2022;172:134–9. https://doi.org/10.1016/j.radonc.2022.05.015.

[13] Sørensen BS, Bassler N, Nielsen S, Horsman MR, Grzanka L, Spejlborg H, et al. Relative biological effectiveness (RBE) and distal edge effects of proton radiation on early damage in vivo. Acta Oncol 2017;56:1387–91. https://doi.org/10.1080/0284186X.2017.1351621.

[14] Saager M, Peschke P, Brons S, Debus J, Karger CP. Determination of the proton RBE in the rat spinal cord: is there an increase towards the end of the spread-out Bragg peak? Radiother Oncol 2018;128:115–20. https://doi.org/10.1016/j.radonc.2018.03.002.

[15] Szabó ER, Brand M, Hans S, Hideghéty K, Karsch L, Lessmann E, et al. Radiobiological effects and proton RBE determined by wildtype zebrafish embryos. PLoS One 2018;13:e0206879.

[16] Horst F, Bodenstein E, Brand M, Hans S, Karsch L, Lessmann E, et al. Dose and dose rate dependence of the tissue sparing effect at ultra-high dose rate studied for proton and electron beams using the zebrafish embryo model. Radiother Oncol 2024;194:110197. https://doi.org/10.1016/j.radonc.2024.110197.

[17] Sørensen BS. Commentary: RBE in proton therapy–where is the experimental in vivo data? Acta Oncol 2019;58:1337–9. https://doi.org/10.1080/0284186X.2019.1669819.

[18] Bahn E, Bauer J, Harrabi S, Herfarth K, Debus J, Alber M. Late contrast enhancing brain lesions in proton-treated patients with low-grade glioma: clinical evidence for increased periventricular sensitivity and variable RBE. Int J Radiat Oncol Biol Phys 2020;107:571–8. https://doi.org/10.1016/j.ijrobp.2020.03.013.

[19] Ödén J, Toma-Dasu I, Witt Nyström P, Traneus E, Dasu A. Spatial correlation of linear energy transfer and relative biological effectiveness with suspected treatment-related toxicities following proton therapy for intracranial tumors. Med Phys 2020;47:342–51. https://doi.org/10.1002/mp.13911.

[20] Peeler CR, Mirkovic D, Titt U, Blanchard P, Gunther JR, Mahajan A, et al. Clinical evidence of variable proton biological effectiveness in pediatric patients treated for ependymoma. Radiother Oncol 2016;121:395–401. https://doi.org/10.1016/j.radonc.2016.11.001.

[21] Niemierko A, Schuemann J, Niyazi M, Giantsoudi D, Maquilan G, Shih HA, et al. Brain necrosis in adult patients after proton therapy: is there evidence for dependency on linear energy transfer? Int J Radiat Oncol Biol Phys 2021;109:109–19. https://doi.org/10.1016/j.ijrobp.2020.08.058.

[22] Fjæra LF, Indelicato DJ, Handeland AH, Ytre-Hauge KS, Lassen-Ramshad Y, Muren LP, et al. A case-control study of linear energy transfer and relative biological effectiveness related to symptomatic brainstem toxicity following pediatric proton therapy. Radiother Oncol 2022;175:47–55. https://doi.org/10.1016/j.radonc.2022.07.022.

[23] Handeland AH, Indelicato DJ, Fjæra LF, Ytre-Hauge KS, Pettersen HES, Muren LP, et al. Linear energy transfer-inclusive models of brainstem necrosis following proton therapy of paediatric ependymoma. Phys Imaging Radiat Oncol 2023;27:100466. https://doi.org/10.1016/j.phro.2023.100466.

[24] Safai S, Trofimov A, Adams JA, Engelsman M, Bortfeld T. The rationale for Intensity-modulated proton therapy in geometrically challenging cases. Phys Med Biol 2013;58:6337–53. https://doi.org/10.1088/0031-9155/58/18/6337.

[25] Giantsoudi D, Adams J, MacDonald S, Paganetti H. Can differences in linear energy transfer and thus relative biological effectiveness compromise the dosimetric advantage of intensity-modulated proton therapy as compared to passively scattered proton therapy? Acta Oncol 2018;57:1259–64. https://doi.org/10.1080/0284186X.2018.1468090.

[26] Giantsoudi D, Adams J, MacDonald SM, Paganetti H. Proton treatment techniques for posterior fossa tumors: consequences for linear energy transfer and dose-volume parameters for the brainstem and organs at risk. Int J Radiat Oncol Biol Phys 2017;97:401–10. https://doi.org/10.1016/j.ijrobp.2016.09.042.

[27] Fjæra LF, Li Z, Ytre-Hauge KS, Muren LP, Indelicato DJ, Lassen-Ramshad Y, et al. Linear energy transfer distributions in the brainstem depending on tumour location in intensity-modulated proton therapy of paediatric cancer. Acta Oncol 2017;56:763–8. https://doi.org/10.1080/0284186X.2017.1314007.

[28] Hahn C, Eulitz J, Peters N, Wohlfahrt P, Enghardt W, Richter C, et al. Impact of range uncertainty on clinical distributions of linear energy transfer and biological effectiveness in proton therapy. Med Phys 2020;47:6151–62. https://doi.org/10.1002/mp.14560.

[29] Toussaint L, Matysiak W, Alapetite C, Aristu J, Bannink-Gawryszuk A, Bolle S, et al. Clinical practice in European centres treating paediatric posterior fossa tumours with pencil beam scanning proton therapy. Radiother Oncol 2024:110414. https://doi.org/10.1016/j.radonc.2024.110414.

[30] Kalholm F, Grzanka L, Traneus E, Bassler N. A systematic review on the usage of averaged LET in radiation biology for particle therapy. Radiother Oncol 2021;161:211–21. https://doi.org/10.1016/j.radonc.2021.04.007.

[31] Hahn C, Ödén J, Dasu A, Vestergaard A, Fuglsang Jensen M, Sokol O, et al. Towards harmonizing clinical linear energy transfer (LET) reporting in proton radiotherapy: a European multi-centric study. Acta Oncol 2022;61:206–14. https://doi.org/10.1080/0284186X.2021.1992007.

[32] Mahajan A, Stavinoha PL, Rongthong W, Brodin NP, McGovern SL, El Naqa I, et al. Neurocognitive effects and necrosis in childhood cancer survivors treated with radiation therapy: a PENTEC comprehensive review. Int J Radiat Oncol Biol Phys 2021;S0360–3016(21):00127–9. https://doi.org/10.1016/j.ijrobp.2020.11.073.

[33] Unkelbach J, Botas P, Giantsoudi D, Gorissen BL, Paganetti H. Reoptimization of intensity modulated proton therapy plans based on linear energy transfer. Int J Radiat Oncol Biol Phys 2016;96:1097–106. https://doi.org/10.1016/j.ijrobp.2016.08.038.

[34] McNamara AL, Schuemann J, Paganetti H. A phenomenological relative biological effectiveness (RBE) model for proton therapy based on all published in vitro cell survival data. Phys Med Biol 2015;60:8399–416. https://doi.org/10.1088/0031-9155/60/21/8399.

[35] Otterlei OM, Indelicato DJ, Toussaint L, Ytre-Hauge KS, Pilskog S, Fjaera LF, et al. Variation in relative biological effectiveness for cognitive structures in proton therapy of pediatric brain tumors. Acta Oncol 2021;60:267–74. https://doi.org/10.1080/0284186X.2020.1840626.

[36] Handeland AH, Lægdsmand PM, Toussaint L, Stokkevåg CH, Lassen-Ramshad YA, Klitgaard R, et al. Linear energy transfer-inclusive brainstem necrosis risk models applied to an independent paediatric proton therapy cohort. Acta Oncol 2023;62:1536–40. https://doi.org/10.1080/0284186X.2023.2254476.

[37] Wagenaar D, Schuit E, van der Schaaf A, Langendijk JA, Both S. Can the mean linear energy transfer of organs be directly related to patient toxicities for current head and neck cancer intensity-modulated proton therapy practice? Radiother Oncol 2021;165:159–65. https://doi.org/10.1016/j.radonc.2021.09.003.

[38] McMahon SJ. Proton RBE models: commonalities and differences. Phys Med Biol 2021;66:04NT02. https://doi.org/10.1088/1361-6560/abda98.

[39] Kalholm F, Grzanka L, Toma-Dasu I, Bassler N. Modeling RBE with other quantities than LET significantly improves prediction of in vitro cell survival for proton therapy. Med Phys 2023;50:651–9. https://doi.org/10.1002/mp.16029.